

Scattering of light by spin waves of the low-frequency branch of the spectrum in weakly ferromagnetic CoCO_3

A. S. Borovik-Romanov, V. G. Zhotikov, and N. M. Kreines

Institute of Physical Problems, Academy of Sciences, USSR
(Submitted 23 January 1978)
Zh. Eksp. Teor. Fiz. 74, 2286–2299 (June 1978)

The low-frequency part of the spin-wave spectrum in weakly ferromagnetic CoCO_3 at $T \lesssim 2$ K is investigated by the single-magnon Mandel'shtam-Brillouin light-scattering method. Scattering of light by magnons propagating both perpendicular and parallel to the external magnetic field is observed for the first time. The contribution to the spectrum produced by magnetic dipole interaction is isolated. The AFMR parameters γ and H_D and the velocities of spin waves along the C_3 axis and in the basal plane of the crystal are determined. The velocities of transverse and longitudinal sound at $T = 300$ K are found for the same directions.

PACS numbers: 75.30.Ds, 75.50.Dd, 78.35.+c

1. INTRODUCTION

Experiments on observation of light scattering by spin waves in magnetically ordered materials were first performed by Fleury and coworkers.^[1] What was observed in these experiments was two- and one-magnon scattering by magnon branches with an appreciable gap ($3\text{--}5\text{ cm}^{-1}$) in the energy spectrum.

In recent years there have appeared in the literature a number of papers of Sandercock and coworkers, devoted to the study of one-magnon Mandel'shtam-Brillouin scattering (OMBS) of light by the low-frequency branch of the magnon spectrum^[2-5] by means of a Fabry-Perot interferometer. The low intensity of light scattering by low-energy magnons and the large background signal from scattering by the defects present in real crystals necessitate use of interferometers with large contrast ($>10^5\text{--}10^6$). Such contrast was achieved in a multi-pass Fabry-Perot interferometer the successful construction of which was worked out by Sandercock^[6] (see also the review article by Fabelinskii and Chisty^[7]). The OMBS method permits investigation of that part of the magnon spectrum where the exchange interaction, the magnetic dipole interaction, and the interaction of the spin system with the magnetic field make approximately equal contributions to the magnon energy, and each of these contributions can be isolated. Thus this method contains within itself the possibilities of magnetic resonance and significantly supplements the information obtainable from neutron diffraction and from two-magnon scattering.

As in the case of scattering by phonons, scattering by magnons occurs because of the modulation of the dielectric permittivity ϵ of the material produced by oscillations of the sublattice magnetizations of the magnet (see, for example, Fabelinskii^[8]). In order to find the components $\Delta\epsilon^{ij}$ of the alternating part of the permittivity tensor, one must know how ϵ varies with the magnetization of the sublattices. In magnetically ordered crystals, the permittivity contains a term dependent on the two ordering vectors: the ferromagnetic (\mathbf{m}) in the case of ferro- and ferrimagnets and the antiferromagnetic (\mathbf{l}) in the case of antiferromagnets (see, for example, Pisarev^[9]). This contribution can

be represented as a series in powers of the appropriate ordering vector: for ferromagnets,

$$\epsilon_j^{ij} = \epsilon_0^{ij} + \alpha_p^{ij} m_p \pm \beta_{pq}^{ij} m_p m_q; \quad (1a)$$

for antiferromagnets,

$$\epsilon_a^{ij} = \epsilon_0^{ij} + \lambda_{pq}^{ij} l_p l_q. \quad (1b)$$

For antiferromagnets with weak ferromagnetism, formula (1b) must be supplemented with a term linear in \mathbf{l} (or, equivalently, in \mathbf{m}). From symmetry considerations,^[10] a term linear in m_j must make a contribution to the imaginary part of the permittivity tensor and describes the well-known Faraday effect. Quadratic terms go into the real part of the tensor and lead to magnetic birefringence. A spin wave in an antiferromagnet is described by oscillations of both vectors, \mathbf{m} and \mathbf{l} : Δm_i and Δl_i respectively. Hence by linearizing (1a) and (1b) with respect to the variables Δm_i and Δl_i , we can find expressions for the oscillations of the permittivity caused by a spin wave:

$$\Delta\epsilon^{ij} \sim \Delta m_p(r, t), \quad \Delta\epsilon^{ij} \sim \Delta l_p(r, t). \quad (2)$$

Knowing $\Delta\epsilon^{ij}$, one can write (see, for example, Ref. 8) the relation between the amplitudes of the vectors of the incident wave E_{inc} and of the scattered wave E_{scat} :

$$E_{\text{scat}} \sim \sum_j \Delta\epsilon_0^{ij} E_{j\text{inc}}. \quad (3)$$

Thus scattering of light by magnons is determined by magneto-optic effects both of the first and of the second order. The suggestion that second-order magneto-optic effects can also contribute to one-magnon scattering was first made in papers of Hu and Morgenthaler^[11] and of Le Gall *et al.*^[12]

So far, sufficiently detailed investigations have been made of the long-wave part of the magnon spectrum for ferromagnetic CrBr_3 ,^[3] ferrimagnetic yttrium-iron garnet,^[2] and weakly ferromagnetic FeBO_3 .^[4] In all these materials, the intensity of the scattered light is determined by the linear magneto-optic interaction (Faraday effect).

In Ref. 5 we reported preliminary results of a study of the low-frequency branch of the magnon spectrum by the OMBS method in the weakly ferromagnetic crystal

CoCO₃. In contrast to the cases indicated above, in CoCO₃ the scattering occurs because of the existence in the crystal under investigation of a strong magnetic birefringence, which depends significantly on the direction of the antiferromagnetism vector **l**; that is, in this case a second-order magneto-optic effect contributes to the light scattering.

The present paper is devoted to such an investigation of the low-frequency part of the spin-wave spectrum by the OMBS method in CoCO₃, and also an investigation of the spectrum of acoustic phonons in this compound.

2. MAGNETIC AND MAGNETOOPTIC PROPERTIES OF CoCO₃

CoCO₃ is a rhombohedral crystal whose symmetry is described by space group D_{3d}^6 . At $T_N = 18.1$ K, this compound transforms to an ordered antiferromagnetic state with anisotropy of the "easy plane" type. The magnetic moments of the sublattices are canted and form a spontaneous ferromagnetic moment m_s , which lies in the basal plane (111). The magnetic properties of CoCO₃ have been studied in considerable detail both by static methods^[13] and by the method of structural neutron diffraction.^[14] Some characteristics of this compound are given in Table I.

The spin-wave spectrum for a magnetic structure of the CoCO₃ type has been calculated by Borovik-Romanov^[16] and by Turov.^[17] When the magnetic field is applied in the basal plane, this spectrum consists of two branches:

$$(v_1/\gamma)^2 = H(H+H_D) + \alpha_{\parallel}^2 k_{\parallel}^2 + \alpha_{\perp}^2 k_{\perp}^2 + H_{\Delta}^2, \quad (4)$$

$$(v_2/\gamma)^2 = 2H_A H_E + H H_D + \alpha_{\parallel}^2 k_{\parallel}^2 + \alpha_{\perp}^2 k_{\perp}^2. \quad (5)$$

Here H is the external field, H_D , H_E , and H_A are, respectively, the effective Dzyaloshinskii, exchange, and anisotropy fields, γ is the gyromagnetic ratio, α_{\parallel} and α_{\perp} are the exchange constants for spin waves propagated along the trigonal axis and in the basal plane, respectively, \mathbf{k} is the wave vector of the spin wave; and H_{Δ} is an additional gap in the spectrum, which may arise from interaction of the electronic spin system

TABLE I. Crystallographic*, magnetic, and magneto-optical parameters for CoCO₃, MnCO₃, and FeBO₃.

Parameters	CoCO ₃	MnCO ₃	FeBO ₃
Constant d of the rhombohedral cell, Å	5.68	5.84	5.520
Angle α	48.2°	47.3°	49.54°
T_N , K	18.1	32.4	348
$4\pi m_s$, G	647	64.2	179 ($T=77$ K)
H_D , kOe	27	4.4	105 ($T=77$ K)
χ ($T=0$ K), 10^{-3} cgs	1.84	1.17	0.14
emu/cm			
Magnetic birefringence $n_x - n_y$	$2.7 \cdot 10^{-4}$ [1500]** ($\lambda=633$ nm)	$< 10^{-5}$ ($\lambda=633$ nm)	$1 \cdot 10^{-5}$ [80] ($\lambda=514$ nm)
Faraday effect, deg cm ⁻¹	< 100 ($\lambda=633$ nm)	-	2300 ($\lambda=514$ nm)
Natural birefringence $n_o - n_e$ ($T=300$ K)	0.255 [$15.6 \cdot 10^5$]***	0.219 [$13.3 \cdot 10^5$]***	0.058 [$4 \cdot 10^5$] ($\lambda=514$ nm)

*Space group D_{3d}^6 .

**The values in deg/cm are given in square brackets.

***The data given refer to $\lambda=589$ nm and are taken from Ref. 15.

with various other degrees of freedom of the crystal (phonons, the nuclear system, etc.). The known results of study of AFMR in CoCO₃^[18-20] indicate that to a sufficient degree of accuracy, $H_{\Delta} = 0$. The absence of a gap in the low-frequency branch (4) of the spectrum permits investigation of it by means of OMBS.

We shall hereafter be interested only in the low-frequency branch of this spectrum.

The presence of a comparatively large ferromagnetic moment in CoCO₃ makes it necessary to take account of magnetic dipole interaction in calculating the long-wave part of the spectrum. A calculation of the spectrum with allowance for this interaction, for antiferromagnets with anisotropy of the easy-plane type, was carried out by Ozhogin^[21] and by Bar'yakhtar *et al.*^[22] In order to present the formulas obtained in these papers in a form convenient for comparison with experiment, we choose a coordinate system such that the z axis coincides with the third-order symmetry axis C_3 and the x and y axes lie in the basal plane; the x axis coincides with the direction of the external magnetic field. For magnons propagating along the x axis ($\mathbf{k} \parallel x$), the spectrum has the form

$$(v/\gamma)^2 = H(H+H_D) + \alpha_{\parallel}^2 k_{\parallel}^2. \quad (6)$$

For y magnons ($\mathbf{k} \parallel y$),

$$(v/\gamma)^2 = H(H+H_D) + 4\pi\kappa(H+H_D)^2 + \alpha_{\parallel}^2 k_{\parallel}^2; \quad (7)$$

for z magnons ($\mathbf{k} \parallel z$),

$$(v/\gamma)^2 = H(H+H_D)(1+4\pi\kappa) + \alpha_{\parallel}^2 k_{\parallel}^2. \quad (8)$$

Here κ is the magnetic susceptibility in the basal plane at $T=0$ K. Allowance for magnetic-dipole interaction leads, in practice, to a significant change only of the spectrum for $k = k_y$. In this branch there is a gap, of amount $(4\pi\kappa)^{1/2} H_D$, in the absence of a magnetic field.

In the paramagnetic state, the CoCO₃ crystal is uniaxial and possesses a quite large natural birefringence (see Table I). On transition to the antiferromagnetic state, there arises in CoCO₃ an additional magnetic birefringence Δn_M due to the appearance of the antiferromagnetic vector \mathbf{l} .^[23] The value of Δn_M includes two contributions: an isotropic, independent of the direction of the antiferromagnetic vector \mathbf{l} , and an anisotropic, dependent on the direction of \mathbf{l} with respect to the crystallographic axes. In particular, there is a quite large difference $n_x - n_y$ of the indices of refraction for light propagating along the trigonal axis of the crystal, amounting to ~ 1500 deg/cm (at $\lambda = 632.8$ nm), and the crystal becomes optically biaxial. But $n_x - n_y$ is small in comparison with the natural birefringence $n_o - n_e$, and the angle between the new optic axes is also small ($\sim 3^\circ$ ^[24]). We have observed no noticeable Faraday rotation (larger than 100 deg/cm) in CoCO₃. The magneto-optic constants of CoCO₃ are given in Table I; the magnetic part of the dielectric permittivity tensor of this crystal has been calculated by Borovik-Romanov *et al.*^[23]

By use of formula (3), we shall write the components of the electric vector of the light scattered by spin waves for a rhombohedral antiferromagnet of the CoCO₃

type. For this purpose it is necessary to calculate the components of the tensor $\Delta\epsilon^{ij}$ in (2). This can be done if one knows an expression for the magnetic part of the permittivity tensor (see Ref. 23) and the geometry of the oscillations of the spin system in the low-frequency branch of the spin waves. A schematic diagram of these oscillations is shown in Fig. 1 of Borovik-Romanov *et al.*^[25] In first approximation, these oscillations can be described as a rocking of the vectors \mathbf{l} and \mathbf{m} in the basal plane. During such a rocking, \mathbf{m} and \mathbf{l} remain mutually perpendicular. Thus spin waves of the low-frequency mode are described by oscillations of the components Δl_x and Δm_y . In CoCO_3 , according to Ref. 23, the magneto-optic effect is determined by the vector \mathbf{l} ; therefore in a description of light scattering, it is necessary to consider only the component Δl_x . On linearizing the components of the magnetic part of the permittivity tensor (see Ref. 23) with respect to the spin-wave amplitude Δl_x , we obtain expressions for the tensor $\Delta\epsilon$ and, by means of formula (3), for the components of the electric vector of a light wave scattered by a spin wave by virtue of the anisotropic birefringence ($l_0 = 2M_0$ is the doubled magnetization of the sublattices):

$$\begin{pmatrix} E_{x\text{scat}} \\ E_{y\text{scat}} \\ E_{z\text{scat}} \end{pmatrix} \sim \begin{pmatrix} 0 & 2\lambda_r l_0 \Delta l_x & \lambda_a l_0 \Delta l_x \\ 2\lambda_r l_0 \Delta l_x & 0 & 0 \\ \lambda_a l_0 \Delta l_x & 0 & 0 \end{pmatrix} \begin{pmatrix} E_{x\text{inc}} \\ E_{y\text{inc}} \\ E_{z\text{inc}} \end{pmatrix}. \quad (9)$$

In the case of FeBO_3 , which has a magnetic structure similar to that of CoCO_3 , light scattering by spin waves is due to the large Faraday effect.^[4] In this case, the amplitude of a spin wave is determined by the value of Δm_y . Allowing for this fact, and knowing the general form of the tensor for the Faraday effect (see, for example, Ref. 10), we can write an expression for the components of the electric field vector of a light wave scattered by virtue of the Faraday effect:

$$\begin{pmatrix} E_{x\text{scat}} \\ E_{y\text{scat}} \\ E_{z\text{scat}} \end{pmatrix} \sim \begin{pmatrix} 0 & 0 & -i\Phi\Delta m_y \\ 0 & 0 & 0 \\ i\Phi\Delta m_y & 0 & 0 \end{pmatrix} \begin{pmatrix} E_{x\text{inc}} \\ E_{y\text{inc}} \\ E_{z\text{inc}} \end{pmatrix}. \quad (10)$$

Here Φ is the Faraday-rotation constant. Consideration of formulas (9) and (10) shows that in scattering by a spin wave there always occurs a rotation of the plane of polarization of the light by 90° .

3. METHOD AND SPECIMENS

Our scattering experiments^[5] were carried out on CoCO_3 in a 90-degree geometry; that is, we investigated the spectrum of light scattered at angle 90° to the incident beam. In this case, the wave vector of the scattering quasiparticle is $k = 2.5 \cdot 10^5 \text{ cm}^{-1}$ when the wavelength of the incident light is $\lambda = 632.8 \text{ nm}$. The spectral composition of the scattered light was investigated with a high-contrast three-pass scanning Fabry-Perot interferometer of the American firm "Burleigh," manufactured according to the principle described by Sandercock.^[6] This interferometer possesses contrast $\sim 10^7 - 10^8$. The scanning is accomplished in it by means of a piezoceramic, to which is fed a saw-toothed voltage. Control of the interferometer and automatic ad-

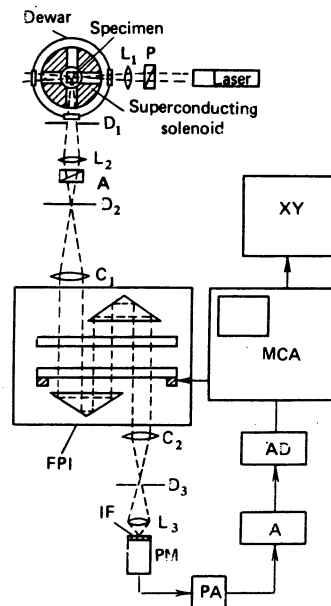


FIG. 1. Schematic diagram of experimental setup for observation of light scattered at angle 90° to the incident beam: L_1 , L_2 , L_3 , lenses; D_1 , D_2 , D_3 , diaphragms; P, polarizer; A, analyzer; C_1 , C_2 , collimating systems; FPI, Fabry-Perot interferometer; IF, interference filter; PA, preamplifier; A, amplifier; AD, amplitude discriminator; MCA, multichannel analyzer; XY, xy-recorder; PM, photomultiplier.

justment are carried out with a DAS-1 system manufactured by the same firm.

The light source in all the experiments was a helium-neon laser LG-36A with $\lambda = 632.8 \text{ nm}$ and power $\sim 50 \text{ mW}$. A detailed schematic of the experimental setup—its optical and recording parts—is shown in Fig. 1. The light scattered in the specimen at angle 90° to the incident beam is collected by lens L_2 at diaphragm D_2 (diameter $\sim 1 \text{ mm}$), which is located at the focus of the collimating system C_1 ($f = 400 \text{ mm}$). The parallel beam of light that leaves this system falls on the interferometer and, on leaving it, is focused by the collimating system C_2 ($f = 250 \text{ mm}$) at the diaphragm D_3 (diameter $\sim 1 \text{ mm}$) and then, through the auxiliary lens L_3 , falls on the photocathode of the cooled FEU-79 photomultiplier. In investigation of the polarization of the scattered light, the necessary polarizing prisms (denoted in Fig. 1 by P and A) were placed in the incident and scattered beams. The recording of the signal from the photodetector was carried out with a photon-counting circuit. The signal from the photomultiplier passed through a preamplifier (PA) to an amplifier-discriminator unit, which gave out shaped pulses of duration $\sim 6 \text{ nsec}$. For matching with the analyzer input section, these pulses were lengthened to 20 nsec and fed to the multichannel spectral analyzer located in the DAS-1 system. This analyzer was synchronized with the scanning frequency of the interferometer. The spectrum accumulated at the DAS-1 system was recorded on an xy-recorder, or else the parameters of this spectrum (position and intensity of the lines) were read with the DAS-1 display.

The scattering experiments were performed both at

room temperature (for investigation of phonons) and at $T \sim 1.5-2.0$ K in a bath of superfluid helium (magnons), in an optical cryostat. The magnetic field was produced by superconducting solenoids of various constructions and could be applied along various directions. Light was fed to the specimen through a window in the cryostat and a special aperture in the superconducting coils.

All the scattering experiments made use of a single CoCO_3 specimen,¹⁾ which had the form of a rectangular parallelepiped with base 1×1.2 mm and height 1.8 mm. The z axis (C_3) was directed along a diagonal of the base. This specimen was used to observe scattering by phonons and magnons propagating along three axes in the crystal: x , y , and z . In the geometry shown in Fig. 2, scattering by phonons and by spin waves with $k = k_x$ was observed. By rotation of the crystal through 90° , it was possible to observe scattering by phonons and magnons propagating in the basal plane. In the latter case, if the magnetic field is directed along the height of the parallelepiped, magnons with $k = k_y$ are investigated; but if the magnetic field lies in the plane of the base of the parallelepiped, magnons with $k = k_x$ are investigated.

The errors of determination of the frequency in the spectrum of the scattered light depend on the intensity of the lines. In the best case the error amounted to 0.2 GHz, in the worst to 0.6 GHz. The largest error in the determination of the spin-wave spectrum is determined by uncertainty in the value of the demagnetizing factor, because the specimen did not have the shape of an ellipsoid. This problem is discussed in more detail in the next section.

4. EXPERIMENTAL RESULTS

We shall now discuss the results obtained on scattering of light in CoCO_3 by phonons and magnons.

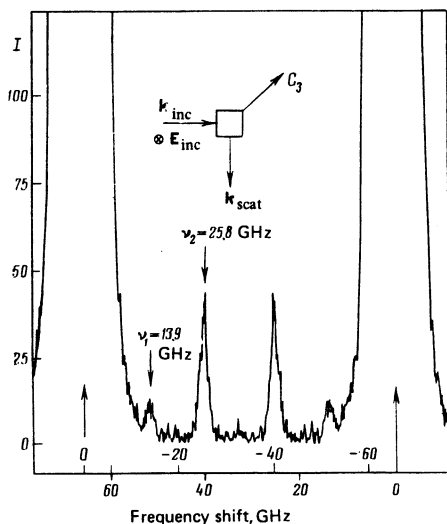


FIG. 2. Spectrum of light ($\lambda = 632.8$ nm) scattered at 90° by phonons propagating along the axis C_3 in CoCO_3 at $t \approx 300$ K. The intense peaks correspond to zero frequency shift and are due to elastic scattering of light by crystal defects. ν_1 corresponds to scattering by a transverse phonon, ν_2 by a longitudinal (the intensity is given in number of counts in 1 sec).

TABLE II. Velocity of sound waves in CoCO_3 .

	v, km/sec	
	Axis C_3 , ([111])	Basal plane, [112]
Longitudinal sound	6.6 ± 0.1	8.2 ± 0.1
Transverse sound	3.7 ± 0.1	4.2 ± 0.1

A. *Phonons*. We studied Mandel'shtam-Brillouin scattering of light by phonons at $T \sim 300$ K in two geometries of the experiment: by phonons propagating along the C_3 axis ([111]) and in the basal plane of the crystal. Figure 2 shows an illustrative record of a spectrum of scattering by phonons propagating along the axis C_3 (the z axis). Two satellites were observed, with frequencies

$$\nu_1^{\text{phz}}(300 \text{ K}) = 13.9 \text{ GHz}, \quad \nu_2^{\text{phz}}(300 \text{ K}) = 25.8 \text{ GHz},$$

corresponding to scattering by transverse and longitudinal phonons. The satellite with frequency ν_1^{phz} is observed for arbitrary mutually perpendicular directions of polarization of the light in the incident and scattered waves. The satellite with frequency ν_2^{phz} is observed only when the polarizations of the incident and scattered light are parallel. Lowering of the specimen temperature to ~ 100 K leads to a slight increase of the satellite frequencies:

$$\nu_1^{\text{phz}}(100 \text{ K}) = 14.6 \text{ GHz}, \quad \nu_2^{\text{phz}}(100 \text{ K}) = 26.1 \text{ GHz}.$$

In the basal plane σ , in direction $[11\bar{2}]$, there are also two satellites in the scattering spectrum. At $T \sim 300$ K their frequencies are

$$\nu_1^{\text{ph}\sigma}(300 \text{ K}) = 16.9 \text{ GHz}, \quad \nu_2^{\text{ph}\sigma}(300 \text{ K}) = 32.4 \text{ GHz}.$$

The polarization conditions for observation of these satellites are the same as in the preceding case. Lowering of the specimen temperature to ~ 100 K produces no change of frequency of these phonons.

By use of the dispersion law for phonons,

$$2\pi\nu = vk_{\text{ph}} \quad (11)$$

(ν is the frequency of the phonon, v is its velocity, and k_{ph} is the wave vector, in our case $2.5 \cdot 10^5 \text{ cm}^{-1}$), we determined the velocities of propagation of longitudinal and transverse sound in the directions investigated. The values obtained are shown in Table II. We did not investigate anisotropy of the sound velocity in the basal plane. This is the first time that data on sound velocity in CoCO_3 have been obtained.

B. *Magnons*. We studied scattering of light by magnons of the low-frequency branch of the spin-wave spectrum for three directions of their wave vector: $\mathbf{k} \parallel \mathbf{x}, \mathbf{y}, \mathbf{z}$. The investigations were carried out over the magnetic-field range 0–4 kOe. Figure 3 shows an illustrative record of a spectrum of light scattered by magnons propagating along the z axis (C_3). It is in this direction that the greatest intensity of scattering is observed. The smallest intensity is observed for scattering by magnons with $k = k_x$. The ratio of these values is ~ 10 . For all three directions, the greatest intensity of the

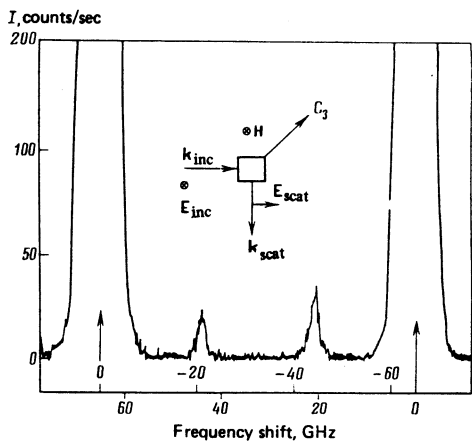


FIG. 3. Spectrum of light ($\lambda = 632.8$ nm) scattered at 90° in CoCO_3 ($T \leq 2$ K) by magnons propagating along the axis C_3 . The peaks shifted by ± 22 GHz correspond to inelastic scattering by magnons.

peaks is observed with scattering in small magnetic fields. With increase of the field, it drops. Because of the small magnitude of the signals, we did not succeed in establishing a quantitative law for the variation of the intensity of the scattering with the value of the magnetic field. Experiment showed that in scattering by y and z magnons there is a rotation of the plane of polarization of the light wave: that is, $E_{\text{scat}} \perp E_{\text{inc}}$. For x magnons, we did not determine the direction of E_{scat} because of the small magnitude of the scattered signal.

The results obtained for the spectra of scattering by magnons in various fields and orientations justify the statement that to within accuracy $\sim 20\%$, the intensities of the Stokes and anti-Stokes components of the spectrum are the same.

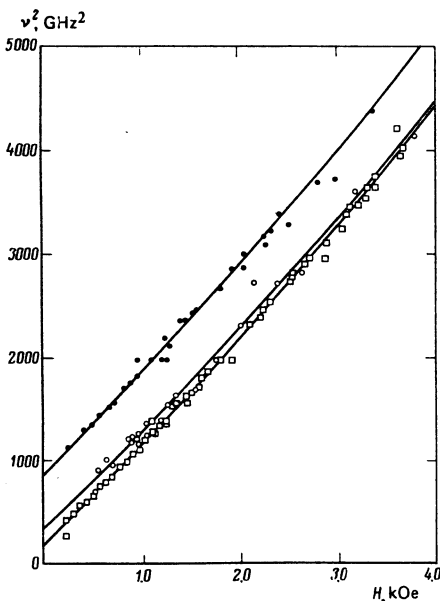


FIG. 4. Variation of the square of the magnon frequency with magnetic field for three directions of propagation of the magnons in a CoCO_3 crystal; \square , k_x along axis C_3 [111]; \circ , k_x in the basal plane, along the magnetic field; \bullet , k_y in the basal plane, perpendicular to the magnetic field; $k = 2.5 \cdot 10^5 \text{ cm}^{-1}$. The solid curves are plotted according to formulas (6)–(8).

Figure 4 shows the variation of the square of the magnon frequency with the value of the internal (that is, with allowance for the demagnetizing factor) magnetic field, for all three directions of the wave vector: k_x , k_y , and k_z . Over the magnetic-field range used in our work, 0–4 kOe, the magnetization of the specimen is practically entirely determined by the spontaneous moment, and the paramagnetic contribution can be neglected. When the magnetic field was applied along the long edge of the crystal parallelepiped and coincided in direction with the magnetization, the demagnetizing factor N was calculated according to formulas given by Joseph and Schlömann^[26] for a rectangular parallelepiped and was taken as 2.2; the demagnetizing field amounted to $\Delta H_1 = 100$ Oe. This geometry was used for all the spectra for magnons with $k = k_y$, and about half the spectra for magnons with $k = k_x$.

In order to observe magnons with $k = k_x$, the magnetic field was directed parallel to a short edge of the parallelepiped (perpendicular to the incident light beam), at angle 45° to the basal plane of the crystal. Some of the spectra for magnons with $k = k_x$ were also taken in a similar configuration. In this case, the direction of the magnetic field did not coincide with the direction of the magnetization, and the formulas of Ref. 26 could not be used. We therefore determined the value of the demagnetizing field in this geometry by mutual agreement of the experimental data for magnons with $k = k_x$ for two directions of the magnetic field: vertical and horizontal. For the demagnetizing field in this configuration, we got the value $\Delta H_2 = 200$ Oe (this corresponds to $N = 5$).

The intensity of the peaks was greatest for magnons with $k \parallel z$. Therefore, as is seen from Fig. 4, the spread of the points was less for this case than for the other two directions. In agreement with formula (8), the points obtained were approximated by the parabola

$$\nu^2 = A_1 + A_2 H + A_3 H^2.$$

By the method of least squares, the following values of the parameters were obtained:

$$A_1 = 187 \pm 60 \text{ GHz}^2, \quad A_2 = 927 \pm 70 \text{ GHz}^2/\text{kOe}, \quad A_3 = 34.5 \pm 18 \text{ GHz}^2/\text{kOe}^2.$$

Hence, in accordance with formula (8), by use of the value of κ given in Table I, we found

$$H_D = 27 \pm 16 \text{ kOe}, \quad \gamma = 5.8 \pm 1.5 \text{ GHz/kOe}, \quad (12)$$

and further

$$\alpha_x = (0.94 \pm 0.3) \cdot 10^{-5} \text{ cm}. \quad (13)$$

By means of these values of H_D and γ and of κ from Table I, we calculated for each of the points obtained for $k = k_x$ the value of

$$(\alpha_x k_x)^2 = (\nu/\gamma)_{\text{calc}}^2 - (\nu/\gamma)_{\text{exp}}^2.$$

Thus the following mean value was obtained:

$$\alpha_x = (1.24 \pm 0.06) \cdot 10^{-5} \text{ kOe} \cdot \text{cm}. \quad (14)$$

In similar manner, for $k = k_y$ we found

$$\alpha_y = (1.18 \pm 0.06) \cdot 10^{-5} \text{ kOe} \cdot \text{cm}. \quad (15)$$

The cited errors in the values of α_x and α_y are rela-

TABLE III. Parameters of the spin-wave spectrum.

Spectrum parameters	CoCO ₃ (T ≈ 2 K)	MnCO ₃ (T = 4,2 K)	FeBO ₃ (T = 77 K)
<i>g</i> -factor	4.0 ^[18] • 2.9 ^[19] • 4.1**	2.0 ^[29] •	2.0 ^[27] • 2.0 ^[4] **
<i>H_D</i> , kOe	27 ^[13] *** 27 ^[18] • 51.5 ^[19] • 0.94**	4.4 ^[16] ***	105 ^[27] *** 105 ^[4] **
α_x , 10 ⁻⁵ kOe · cm		0.88 ^[28] **** 0.79 ^[30] •	7.7 ^[4] **
α_y , 10 ⁻⁵ kOe · cm	1.21**	0.63 ^[28] ****	6.3 ^[4] **
2 $\pi\gamma\alpha_x$, km/sec	3.43**	1.55 ^[28] ****	13.51 ^[4] **
2 $\pi\gamma\alpha_y$, km/sec	4.38**	1.11 ^[28] ****	11.18 ^[4] **
<i>H_E</i> , kOe	240**	224.5 ^[28] ****	1990 ^[4] **
<i>H_E</i> [⊥] , kOe	310**	461.02 ^[28] ****	4650 ^[4] **
<i>J₁</i> + <i>J₂</i> , GHz	-71.2**	-31.9 ^[28] ****	-297 ^[4] **
<i>J₁</i> - <i>J₂</i> , GHz	-45.4**	+0.7 ^[28] ****	-12 ^[4] **

*From data on AFMR and parametric excitation of spin waves.
**From optical data.
***From static magnetic measurements.
****From neutron-diffraction data.

tive errors of the joint determination of all three exchange constants α_x , α_y and α_z . The error in the absolute values of α_x and α_y is one and a half times as large as for α_z because of the larger spread of the points for magnons of these directions. The agreement of the values of α_x and α_y within the limits of relative error, as should be the case according to the theory of spin waves (see below), confirms the correctness of the expression derived by Ozhogin^[21] and by Bar'yakhtar *et al.*^[22] for the energy of dipole interaction of spin waves [formula (7)].

The solid curves in Fig. 4 are drawn according to formulas (6)–(8) with the values of the constants quoted above. The values we obtained for the parameters of the magnon spectrum for CoCO₃ are shown in Table III (here $\alpha_1 = (\alpha_x + \alpha_y)/2$). Given in the same table, for comparison, are the parameters of the spin-wave spectrum for FeBO₃, determined from experiments with OMBS^[4] and AFMR,^[27] and for MnCO₃, determined from experiments with neutron scattering^[28] and AFMR.^[29] Such a comparison is interesting because all three materials have the same crystalline and magnetic structures.

5. DISCUSSION OF RESULTS

A. The experiments with OMBS enabled us to determine the AFMR parameters γ and *H_D*. Our values (see Table III) agree better with the data of Rudashevskii^[18] than with the data of Prozorova *et al.*^[19] But in discussing this discrepancy, we must remark that the values of $\gamma^2 H_D$, which basically determine the field dependence of the magnon frequency, agree much better: 847 GHz²/kOe in Ref. 18, 1090.7 GHz²/kOe in Ref. 19, and 906 GHz²/kOe in our measurements. A reason for the discrepancy may also be the fact that there is a gap in the AFMR spectrum.

B. Our experiments include the first successful observation of scattering by magnons propagating along three principal directions in the crystal: $\mathbf{k} \parallel \mathbf{x}$ (*k_x*), \mathbf{y} (*k_y*), and \mathbf{z} (*k_z*). For FeBO₃,^[4] because of the geometry of the experiment, only *k_y* and *k_z* magnons were

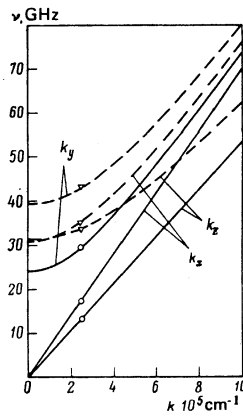


FIG. 5. Low-frequency part of the spin-wave spectrum $\nu(k)$ for CoCO₃, plotted according to formulas (6)–(8) with use of the constants determined in this paper. The solid curves correspond to zero external field, the dotted to *H* = 1 kOe. The points denote the experimental values obtained for $k = 2.5 \cdot 10^5 \text{ cm}^{-1}$.

investigated. The agreement of our data with formulas (6) and (8) has confirmed the correctness of the calculation of the dipole contribution to the spin-wave energy of an easy-plane antiferromagnet with weak ferromagnetism.^[21,22] In particular, a difference between it and an isotropic ferromagnet has been detected, consisting in the fact that in the easy-plane antiferromagnet the only spin waves that have large energies are those that propagate in the direction perpendicular to the magnetic field and to the easy axis, namely along the *y* axis. This feature is illustrated in Fig. 5, which shows spin-wave spectra plotted according to formulas (6)–(8), with use of the constants we have determined, for the case in which the external field is zero (solid curves) and for a field of 1 kOe (dotted curves). It is seen from Fig. 5 that the dipole-dipole interaction leads to the result that in zero magnetic field the spectrum of

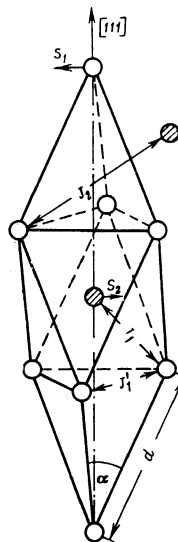


FIG. 6. Crystal structure of rhombohedral crystals of the CoCO₃ type (*D_{3d}*). *S₁* and *S₂* indicate the directions of the spins in the lattice; *J₁*' is the exchange integral of interaction within a sublattice, *J₁* (for nearest neighbors) and *J₂* (for next-nearest neighbors) between the two sublattices.

magnons propagated along the γ axis has a gap of amount 23.7 GHz.

C. We turn now to discussion of the values obtained for the exchange constants α_{\parallel} and α_{\perp} , which determine the velocities of propagation of spin waves. We note (compare Tables II and III) that the latter are close in value to the velocities of propagation of transverse phonons at $T=300$ K in the corresponding directions. It is seen from Table III that the anisotropy of the values of α for CoCO_3 has the opposite sign as compared with FeBO_3 and MnCO_3 . Also noticeable is the anomalously large value of α_{\perp} and α_{\parallel} , although CoCO_3 has the lowest Néel temperature of all three compounds. Some overestimation of our value of α may have resulted from the existence of a gap, so far not observed, in the AFMR spectrum.

By use of spin-wave theory, one can relate the values of α_{\perp} and α_{\parallel} to the values of the exchange-interaction integrals of magnetic ions within a sublattice, J'_1 , and between the two sublattices: J_1 for nearest neighbors and J_2 for next-nearest (see Fig. 6). Calculations by spin-wave theory as applied to a rhombohedral crystal, carried out by Holden *et al.*^[28] and by Wettling, Sandercock, and Jantz,^[4] lead to the following results. The exchange term in the expression for the spin-wave energy has the form

$$v^{(L)} = \alpha_{\parallel(L)}' k_{\parallel(L)} = \gamma H_E^{(L)} k d \cos \theta, \quad (16)$$

where d is the lattice constant, $\alpha' = \gamma\alpha$, k is the absolute value of the wave vector of the spin wave, and θ is the angle between corresponding vectors of the direct and reciprocal lattices ($\theta = 46.9^\circ$ for CoCO_3). The values of the exchange fields are related as follows to the values of the exchange integrals: in the case $k \parallel z$,

$$H_E^{\parallel} = (5/\gamma) (J_1 + J_2) \sec \beta; \quad (17)$$

when $k \perp z$,

$$H_E^{\perp} = (5/\gamma) [(J_1 + J_2) (J_1 + 4J_2 - 3J'_1)]^{1/2} \sqrt{8} \operatorname{cosec} \beta, \quad (18)$$

where β is the angle between the vector of the direct lattice and the z axis ($[111]$). For CoCO_3 , $\beta = 75.03^\circ$. Formulas (16)–(18) were derived on the assumption that k_{\perp} is directed along $[11\bar{2}]$ and that $H_D \ll H_E$, $H_A \ll H_E$. From them it is evident that if the dominant interaction is that with nearest neighbors, the spin-wave velocities and the corresponding exchange fields must be related thus:

$$\alpha_{\parallel}/\alpha_{\perp} = H_E^{\parallel}/H_E^{\perp} = \sqrt{8} \operatorname{tg} \beta. \quad (19)$$

In the case of FeBO_3 and MnCO_3 , the experimental results are close to this value and thus confirm that the principal reason for the anisotropy of the velocity of propagation of spin waves in these materials is the rhombohedral distortion of the lattice.

The anisotropy of the exchange fields in the case of CoCO_3 has an entirely different character. The exchange field along the trigonal axis is 30% smaller than the exchange field in the plane. This means that the values of the exchange integrals for interaction with the second and third coordination spheres are comparable with the first exchange integral. Formulas

(17) and (18) enable us to obtain values for the following combinations of exchange integrals: $J_1 + J_2$ and $J_2 - J'_1$. The values obtained by us and in Refs. 4 and 28 are given in Table III. For CoCO_3 , the value of $J_2 - J'_1$ amounts to more than 30% of $J_1 + J_2$. Noticeable also is the anomalously large value of the exchange integrals in CoCO_3 . Explanation of all these anomalies must be sought in peculiarities of the distribution of the effective spin density of the cobalt ion, whose magnetic moment receives a very large contribution from the orbital motion of the electrons.

In conclusion, the authors express their sincere thanks to P. L. Kapitza for constant interest in the research, and also to S. M. Elagin for help in construction of the apparatus and in the conduct of the experiments.

¹⁾The authors sincerely thank N. Yu. Ikornikova and V. M. Egorov for providing the CoCO_3 specimen.

¹⁾P. A. Fleury, S. P. S. Porto, L. E. Cheesman, and H. J. Guggenheim, *Phys. Rev. Lett.* **17**, 84 (1966); P. A. Fleury, S. P. S. Porto, and R. Loudon, *Phys. Rev. Lett.* **18**, 658 (1967); P. A. Fleury, R. Loudon, and L. R. Walker, *J. Appl. Phys.* **42**, 1649 (1971).

²⁾J. R. Sandercock and W. Wettling, *Solid State Commun.* **13**, 1729 (1973); W. Wettling, M. G. Cottam, and J. R. Sandercock, *J. Phys. C* **8**, 211 (1975).

³⁾J. R. Sandercock, *Solid State Commun.* **15**, 1715 (1974).

⁴⁾W. Jantz, J. R. Sandercock, and W. Wettling, *J. Phys. C* **9**, 2229 (1976).

⁵⁾A. S. Borovik-Romanov, V. G. Zhotikov, N. M. Kreines, and A. A. Pankov, *Pis'ma Zh. Eksp. Teor. Fiz.* **24**, 233 (1976) [*JETP Lett.* **24**, 207 (1976)]; A. S. Borovik-Romanov, V. G. Jotikov, N. M. Kreines, and A. A. Pankov, *Physica* **86-88B**, 1275 (1977).

⁶⁾J. R. Sandercock, *Proc. 2nd Int. Conf. on Light Scattering in Solids*, ed. M. Balkanski, Paris, Flammarion, 1971, p. 9.

⁷⁾I. L. Fabelinskiĭ and I. L. Chistyĭ, *Usp. Fiz. Nauk* **119**, 487 (1976) [*Sov. Phys. Usp.* **19**, 597 (1976)].

⁸⁾I. L. Fabelinskiĭ, *Molekulyarnoe rasseyanie sveta (Molecular Scattering of Light)*, Nauka, 1965. (Translation, Plenum Press, 1968.)

⁹⁾R. S. Pisarev, *Magnitnoe uporyadochenie i opticheskie yavleniya v kristallakh (Magnetic Ordering and Optical Phenomena in Crystals)*, in: *Fizika magnitnykh diélektrikov (Physics of Magnetic Dielectrics)*, L., Nauka, 1974.

¹⁰⁾L. D. Landau and E. M. Lifshitz, *Elektrodinamika sploshnykh sred (Electrodynamics of Continuous Media)*, M., Gostekhzdat, 1957 (translation, Pergamon Press and Addison Wesley, 1960).

¹¹⁾H. L. Hu and F. R. Morgenthaler, *Appl. Phys. Lett.* **18**, 307 (1971).

¹²⁾H. LeGall, J. P. Jamet, and B. Desormiere, *Proc. 2nd Int. Conf. on Light Scattering in Solids*, ed. M. Balkanski, Paris, 1971, p. 170.

¹³⁾A. S. Borovik-Romanov and V. I. Ozhgin, *Zh. Eksp. Teor. Fiz.* **39**, 27 (1960) [*Sov. Phys. JETP* **12**, 18 (1961)]; A. N. Bazhan and N. M. Kreines, *Pis'ma Zh. Eksp. Teor. Fiz.* **15**, 533 (1972) [*JETP Lett.* **15**, 377 (1972)]; A. N. Bazhan, *Zh. Eksp. Teor. Fiz.* **66**, 1086 (1974) [*Sov. Phys. JETP* **39**, 531 (1974)].

¹⁴⁾R. A. Alikhanov, *Zh. Eksp. Teor. Fiz.* **37**, 1145 (1959) [*Sov. Phys. JETP* **10**, 814 (1960)]; P. J. Brown, P. J. Welford, and J. B. Forsyth, *J. Phys. C* **6**, 1405 (1973).

¹⁵⁾A. N. Winchell and H. Winchell, *The Microscopic Characters of Artificial Inorganic Solid Substances: Optical Properties of Artificial Minerals*. 3rd ed., Academic Press, 1964. (Russ. transl., *Opticheskie svoystva iskusstvennykh mineralov (Optical Properties of Artificial Minerals)*, Mir, 1967.

- ¹⁶A. S. Borovik-Romanov, Zh. Eksp. Teor. Fiz. **36**, 766 (1959) [Sov. Phys. JETP **9**, 539 (1959)].
- ¹⁷E. A. Turov, Zh. Eksp. Teor. Fiz. **36**, 1254 (1959) [Sov. Phys. JETP **9**, 890 (1959)].
- ¹⁸E. G. Rudashevskii, Zh. Eksp. Teor. Fiz. **46**, 134 (1964) [Sov. Phys. JETP **19**, 96 (1964)].
- ¹⁹G. D. Bogomolov, Yu. F. Igonin, L. A. Prozorova, and F. S. Rusin, Zh. Eksp. Teor. Fiz. **54**, 1069 (1968) [Sov. Phys. JETP **27**, 572 (1968)].
- ²⁰A. S. Borovik-Romanov and V. F. Meshcheryakov, Pis'ma Zh. Eksp. Teor. Fiz. **8**, 425 (1968) [JETP Lett. **8**, 262 (1968)].
- ²¹V. I. Ozhogin, Zh. Eksp. Teor. Fiz. **48**, 1307 (1965) [Sov. Phys. JETP **21**, 874 (1965)].
- ²²V. G. Bar'yakhtar, M. A. Savchenko, and V. V. Tarasenko, Zh. Eksp. Teor. Fiz. **49**, 1631 (1965) [Sov. Phys. JETP **22**, 1115 (1966)].
- ²³A. S. Borovik-Romanov, N. M. Kreines, A. A. Pankov, and M. A. Talalaev, Zh. Eksp. Teor. Fiz. **66**, 782 (1974) [Sov. Phys. JETP **39**, 378 (1974)].
- ²⁴N. F. Kharchenko, V. V. Eremenko, and O. P. Tutakina, Zh. Eksp. Teor. Fiz. **64**, 1326 (1973) [Sov. Phys. JETP **37**, 672 (1973)].
- ²⁵A. S. Borovik-Romanov, V. G. Zhotikov, N. M. Kreines, and A. A. Pankov, Zh. Eksp. Teor. Fiz. **70**, 1924 (1976) [Sov. Phys. JETP **43**, 1002 (1976)].
- ²⁶R. I. Joseph and E. Schlömann, J. Appl. Phys. **36**, 1579 (1965).
- ²⁷R. C. Le Craw, R. Wolf, and J. W. Nielson, Appl. Phys. Lett. **14**, 352 (1969); E. G. Rudashevskii, V. N. Seleznev, and L. V. Velikov, Solid State Commun. **11**, 959 (1972).
- ²⁸T. M. Holden, E. C. Svenson, and P. Martel, Can. J. Phys. **50**, 687 (1972).
- ²⁹A. S. Borovik-Romanov, N. M. Kreines, and L. A. Prozorova, Zh. Eksp. Teor. Fiz. **45**, 64 (1963) [Sov. Phys. JETP **18**, 46 (1964)].
- ³⁰B. Ya. Kotyuzhanskiy and L. A. Prozorova, Zh. Eksp. Teor. Fiz. **62**, 2199 (1972) [Sov. Phys. JETP **35**, 1150 (1972)].

Translated by W. F. Brown, Jr.

Phase transitions in complex magnetic structures

M. A. Savchenko and A. V. Stefanovich

Moscow Institute of Radio Engineering, Electronics, and Automation

(Submitted 19 December 1977)

Zh. Eksp. Teor. Fiz. **74**, 2300-2310 (June 1978)

High-temperature phase transitions are considered in alloys of rare-earth metals, of the type Er-Tb and Er-Dy, whose magnetic structure is a tilted spiral wave traveling along a preferred axis z of the crystal. For these compounds a phase diagram is constructed in the variables T and $|a_{\parallel}|$ (a_{\parallel} is the anisotropy constant along the z axis); it describes phase transitions from the paramagnetic region to all possible states of the tilted spiral. The discontinuities of the order parameter and the critical exponents are calculated. There is a "tetracritical" point on the phase diagram. The behavior of the system in the vicinity of the "tetracritical" point is considered; and it is shown that in this system, along with first-order phase transitions to a planar spiral or to a state with a longitudinal sinusoidal wave, there can occur a second-order phase transition of the second kind directly to a tilted spiral.

PACS numbers: 75.30.Kz, 75.40.Bw, 64.60.Kw

1. INTRODUCTION

The investigation of phase transitions in magnetic structures such as the helicoidal or sinusoidal (Dy, Er, Ho Tb, Cr, Eu, DyC₂, MnO₂, and REAu₂, where RE represents ions of rare-earth metals) has been the object of a large amount of research.^[1-5] It has been shown that, depending on the symmetry of the system, phase transitions in materials with a complex magnetic structure may be either of first or of second order; the instabilities that lead to phase transitions of the first order are due to fluctuations of the short-range order.

In the present work, we have considered phase transitions in alloys of the type Er-Dy or Er-Tb, in which the magnetic structure is a spiral wave whose plane of polarization is oriented at an arbitrary angle Ψ to the direction of its wave vector q (see Fig. 1), a so-called tilted spiral. A phase diagram for these compounds has been constructed; it describes phase transitions from the paramagnetic region (P) to all possible states of the tilted-spiral structure. On the

phase diagram there is a "tetracritical" point. The renormalization-group (RG) equations describing the behavior of the system near a tetracritical point are derived; and on the basis of these equations, transit-

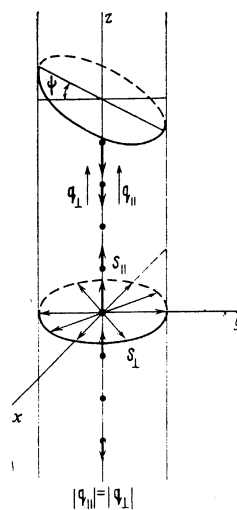


FIG. 1.